

## Gamma-Ray Shielding Capacity of Bi<sub>2</sub>O<sub>3</sub>-SiO<sub>2</sub>-B<sub>2</sub>O<sub>3</sub> Glass Powders with Different Bi<sub>2</sub>O<sub>3</sub> Contents

Aycan SENGUL<sup>1\*</sup>, İskender AKKURT<sup>2</sup>

<sup>1</sup> Akdeniz University, Health Services Vocational School, Medical Imaging Techniques, Antalya, Turkey

<sup>2</sup> Suleyman Demirel University, Science Faculty, Physics Department, Isparta, (ORCID: [0000-0003-4548-5403](https://orcid.org/0000-0003-4548-5403)) (ORCID: [0000-0002-5247-7850](https://orcid.org/0000-0002-5247-7850))



**Keywords:** Monte Carlo simulations, GAMOS, Gamma-ray Shielding, Attenuation coefficient, Bi<sub>2</sub>O<sub>3</sub>-SiO<sub>2</sub>-B<sub>2</sub>O<sub>3</sub> glass powders

### Abstract

The study investigated the shielding properties of Bi<sub>2</sub>O<sub>3</sub>-SiO<sub>2</sub>-B<sub>2</sub>O<sub>3</sub> glass powders with varying Bi<sub>2</sub>O<sub>3</sub> levels (45-60 mass%) against ionizing radiation using GAMOS (version 6.2). The simulation geometry produced by GAMOS was validated by comparing the results to conventional XCOM data for mass attenuation coefficients of glass particles. The Monte Carlo simulations were used to score photons that traveled in an absorber within the energy range of 0.01 MeV to 20 MeV, depending on the parameter under study. The simulation model involved a monoenergetic point source producing a pencil beam, absorber, and detector. We have calculated the mass attenuation coefficient (MAC), Half-value layer (HVL), Tenth-value layer (TVL), and Mean Free Path (MFP). The greatest linear attenuation coefficients in the whole energy range are related to 60Bi and the lowest were to 45Bi. The obtained results were compared, and these results are in good agreement with the obtained values from the XCOM program.

## 1. Introduction

The use of radiation in nuclear technology, medicine, agriculture, and industry has become widespread. As a result, the significance of radiation protection and research on protective materials has increased. To minimize potential radiation exposure, the ALARA principle is applied along with three main rules: time, distance, and shielding. Time and distance are manageable parameters for individuals. However, providing maximum protection from radiation requires investigating various types of materials, compounds, and mixtures for radiation shielding. The literature contains various theoretical, experimental [1]-[10], and simulation evaluations [11]-[23] investigations on shielding materials.

To determine the amount of shielding necessary for a specific target environment, it is necessary to consider the attenuation features of radiation. An absorber's mass attenuation coefficient (MAC) ( $\mu/\rho$ ) indicates the likelihood of a photon

undergoing scatter or absorption interactions per unit distance and unit density of the material. This information is useful in estimating the thickness of a material needed to shield a known type and energy of an ionizing photon beam [24], [25]. The attenuation of material is determined using the transmission method, which follows the Lambert-Beer law. This law is formulated as in Equation 1;

$$\frac{\mu}{\rho} = \left(-\frac{1}{x\rho}\right) \ln\left(\frac{I(x)}{I_0}\right) \quad (1)$$

Where  $I_0$  and  $I_x$  denote the initial and reduced photon intensity, respectively. The variable  $x$  denotes the magnitude of the attenuator material's thickness.

The choice of shielding method primarily relies on the radiation energy and charge characteristics of the shielding materials. The choice of shielding material is contingent upon several factors, such as the nature of the radiation, system specifications, resilience to radiation-induced harm,

\*Corresponding author: [aycansahin@akdeniz.edu.tr](mailto:aycansahin@akdeniz.edu.tr)

Received: 22.12.2023, Accepted: 04.03.2024

economic circumstances, and mechanical characteristics [26]. Low-melting glass is a common binder phase in advanced electronics technology due to its low sealing temperature, heat resistance, and air tightness [27], [28]. PbO-based glasses are particularly popular due to their low glass transition temperature and excellent thermal and electrical properties [29]. Due to the negative effects of lead on health and the environment, many research projects are evaluating lead-free high-density glasses. Several studies on ternary Bi<sub>2</sub>O<sub>3</sub>-containing glass have been undertaken [30]-[33].

The purpose of this study is to compute the gamma-ray shielding parameters of Bi<sub>2</sub>O<sub>3</sub>-SiO<sub>2</sub>-B<sub>2</sub>O<sub>3</sub>-ZnO-Al<sub>2</sub>O<sub>3</sub> glasses. with different Bi<sub>2</sub>O<sub>3</sub> contents are calculated utilizing the GAMOS simulation tool. The computations use Monte Carlo simulations for a wide range of photon energies, and the examined values are compared to XCOM results.

## 2. Material and Method

In problems involving the transport of photons, a Monte Carlo code uses interaction cross sections, along with the geometrical and material descriptions of the medium, to compute estimates of dosimetric quantities such as flux and dose [34], [35].

The investigation utilized the Monte Carlo software package GAMOS 6.2 to model the geometry of the source, absorber, and detector. GAMOS is a CERN-developed derivative of Geant4 commonly used by medical physicists for investigating ionizing

radiation sources in diagnostic or therapeutic contexts [36]. For each sample, representing a separate simulation, photon energies ranging from 0.01 MeV to 20 MeV were studied. All Monte Carlo runs were performed using 10<sup>6</sup> particle histories/tracks, resulting in statistical errors below 0.1%. The simulations did not utilize any variance reduction technique. As seen in figure 1, the simulations involved a mono-energetic photon beam emitted from a pencil beam photon source. The beam was directed towards a disk shape absorber positioned 50 cm away from the source. To prevent any photon interactions with materials other than the sample, all irradiation geometry components were enclosed within a vacuum sphere with a radius of 100 cm.

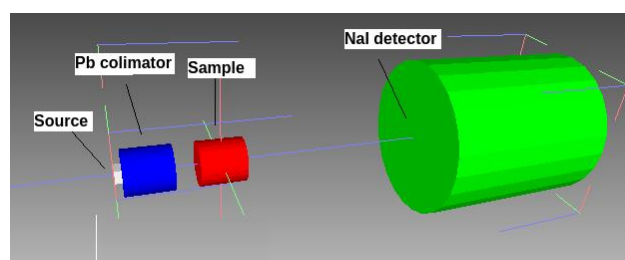


**Figure 1.** GAMOS Simulation geometry obtained with Paraview.

This work investigates the gamma shielding capabilities of four glasses with varying fractions of Bi<sub>2</sub>O<sub>3</sub>, which are significant in radiation protection. Table 1 shows the compositions and densities of each sample.

**Table 1.** Compositions of the Bi<sub>2</sub>O<sub>3</sub>-SiO<sub>2</sub>-B<sub>2</sub>O<sub>3</sub>-ZnO-Al<sub>2</sub>O<sub>3</sub> glasses (mass%).

Sample	$\rho$ (g/cm <sup>3</sup> )	Bi <sub>2</sub> O <sub>3</sub>	SiO <sub>2</sub>	B <sub>2</sub> O <sub>3</sub>	ZnO	Al <sub>2</sub> O <sub>3</sub>
45Bi	5.82	45	10	35	7	3
50Bi	5.93	50	10	30	7	3
55Bi	6.16	55	10	25	7	3
60Bi	6.32	60	10	20	7	3

## 3. Results and Discussion

Four glass samples were performed MAC Monte Carlo tests. The simulations were conducted at twenty-eight different photon intensities, ranging from 0.01 MeV to 20 MeV. The values obtained from the Monte Carlo simulations were inputted into Equation (1) to produce GAMOS code results, which are presented in Table 2.

We calculated the LAC for each sample at different energies, ranging from 0.01 MeV to 20 MeV, using the GAMOS code and XCOM. The

results obtained from both codes were in good agreement with each other.

Figure 2 shows that 60Bi has the highest LAC across the entire energy range, while 45Bi has the lowest. Increasing the amount of Bi<sub>2</sub>O<sub>3</sub> in the material increases its density and therefore its linear attenuation coefficient.

The MAC provides information about the material's performance based on its elemental makeup, regardless of its density. Figure 3 illustrates the variation in  $\mu/\rho$  values in the 0.01-20 MeV energy range.

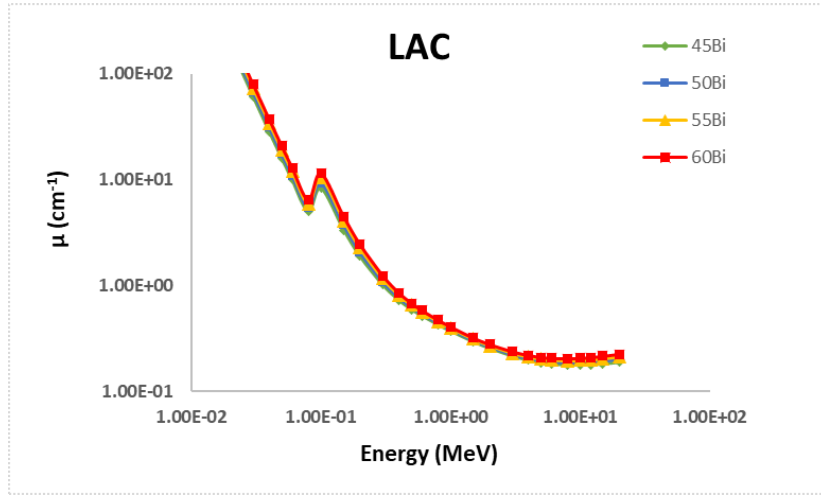


Figure 2. LAC ( $\text{cm}^{-1}$ ) in terms of photon energy for glasses.

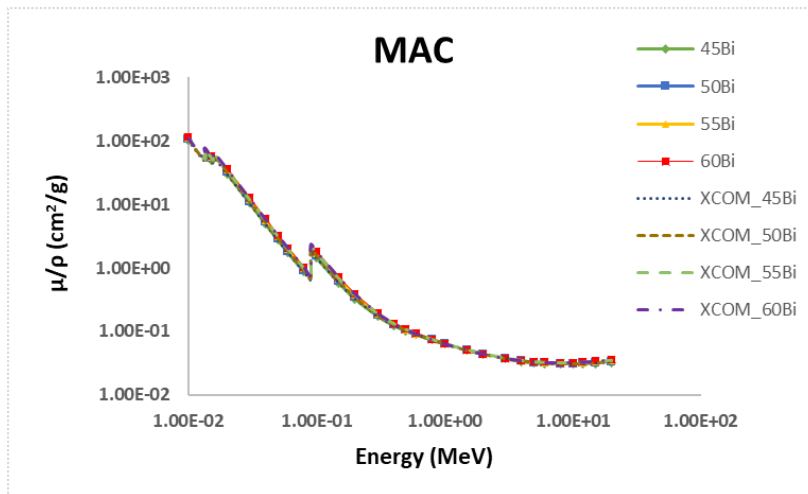


Figure 3. MAC ( $\text{cm}^2/\text{g}$ ) in terms of photon energy for glasses (GAMOS and XCOM).

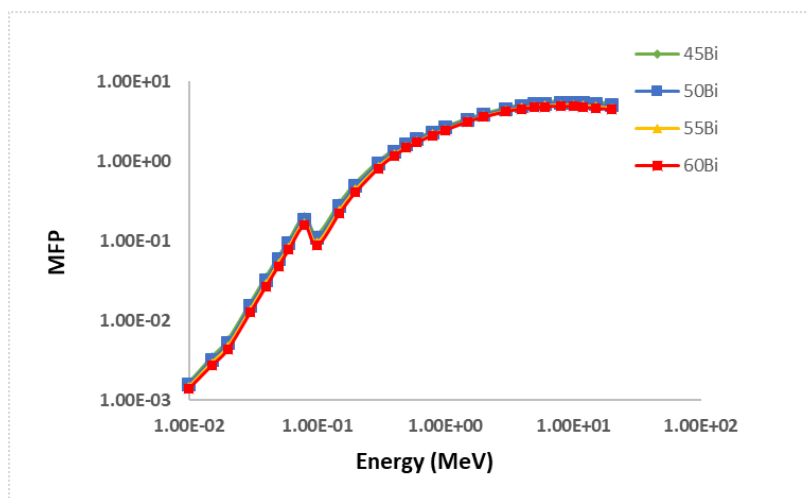


Figure 4. MFP (cm) in terms of photon energy for glasses.

The MFP is an important parameter for evaluating photon shielding characteristics. It refers to the distance that a particle travels between two consecutive collisions, which affects the direction, energy, and other properties of the particle. The MFP is calculated using Equation 2 and is determined by the photon energy, as shown in Figure 4. Increasing the gamma photon energy escalates the MFP of the material. The changes are shown in the energy range of 0.01-20 MeV. At lower energies of 1 MeV, the mean free path (MFP) increases modestly with slope, but at higher energies the slope increases more. The MFP moves relatively smoothly between 0.1 and 1 MeV. As shown in figure 4, 45Bi and 50Bi have a higher average free distance than other materials. This indicates that their materials have less interaction with atoms and may not be the best option for use in shields.

$$MFP = \left(\frac{1}{\mu}\right) \tag{2}$$

The shield thicknesses that reduce the intensity of the incident beam by 50% and 10% are referred to as HVL and TVL, respectively. Equations 3 and 4 are related to LAC.

$$HVL = \left(\frac{\ln 2}{\mu}\right) \tag{3}$$

$$TVL = \left(\frac{\ln 10}{\mu}\right) \tag{4}$$

Radiation shielding is considered adequate when the HVL value is low. Figure 5 shows that HVL and TVL values increase with energy, with 45Bi and 50Bi having the highest values compared to other materials. 60Bi has the lowest value compared to other materials due to its MFP.

**Table 2.** MAC (cm<sup>2</sup>/g) of glasses at various photon energies determined by GAMOS simulation.

Energy (MeV)	45Bi		50Bi		55Bi		60Bi	
	XCOM	GAMOS	XCOM	GAMOS	XCOM	GAMOS	XCOM	GAMOS
0.01	1.03E+02	1.04E+02	1.06E+02	1.07E+02	1.09E+02	1.10E+02	1.12E+02	1.13E+02
0.015	5.02E+01	5.01E+01	5.29E+01	5.27E+01	5.56E+01	5.54E+01	5.83E+01	5.81E+01
0.02	3.07E+01	3.05E+01	3.28E+01	3.26E+01	3.49E+01	3.47E+01	3.70E+01	3.67E+01
0.03	1.05E+01	1.05E+01	1.13E+01	1.12E+01	1.20E+01	1.19E+01	1.27E+01	1.27E+01
0.04	4.93E+00	4.88E+00	5.28E+00	5.22E+00	5.63E+00	5.56E+00	5.97E+00	5.91E+00
0.05	2.76E+00	2.72E+00	2.95E+00	2.91E+00	3.14E+00	3.09E+00	3.34E+00	3.28E+00
0.06	1.74E+00	1.71E+00	1.85E+00	1.83E+00	1.97E+00	1.95E+00	2.09E+00	2.06E+00
0.08	8.69E-01	8.58E-01	9.25E-01	9.12E-01	9.80E-01	9.66E-01	1.04E+00	1.02E+00
0.1	1.44E+00	1.43E+00	1.58E+00	1.56E+00	1.71E+00	1.69E+00	1.84E+00	1.82E+00
0.15	5.78E-01	5.75E-01	6.24E-01	6.21E-01	6.70E-01	6.67E-01	7.16E-01	7.11E-01
0.2	3.28E-01	3.25E-01	3.49E-01	3.46E-01	3.71E-01	3.68E-01	3.92E-01	3.89E-01
0.3	1.74E-01	1.74E-01	1.82E-01	1.81E-01	1.89E-01	1.89E-01	1.96E-01	1.96E-01
0.4	1.25E-01	1.25E-01	1.29E-01	1.28E-01	1.32E-01	1.32E-01	1.36E-01	1.35E-01
0.5	1.03E-01	1.02E-01	1.04E-01	1.04E-01	1.06E-01	1.06E-01	1.08E-01	1.08E-01
0.6	8.90E-02	8.89E-02	9.02E-02	9.01E-02	9.13E-02	9.13E-02	9.25E-02	9.25E-02
0.8	7.32E-02	7.34E-02	7.37E-02	7.39E-02	7.42E-02	7.44E-02	7.47E-02	7.49E-02
1	6.38E-02	6.37E-02	6.40E-02	6.41E-02	6.42E-02	6.44E-02	6.45E-02	6.46E-02
1.5	5.07E-02	5.06E-02	5.07E-02	5.06E-02	5.08E-02	5.07E-02	5.08E-02	5.07E-02
2	4.41E-02	4.39E-02	4.41E-02	4.40E-02	4.42E-02	4.40E-02	4.43E-02	4.41E-02
3	3.73E-02	3.71E-02	3.75E-02	3.72E-02	3.77E-02	3.74E-02	3.79E-02	3.77E-02
4	3.41E-02	3.39E-02	3.44E-02	3.41E-02	3.47E-02	3.44E-02	3.49E-02	3.47E-02
5	3.23E-02	3.22E-02	3.27E-02	3.26E-02	3.31E-02	3.30E-02	3.35E-02	3.33E-02
6	3.13E-02	3.12E-02	3.18E-02	3.17E-02	3.22E-02	3.22E-02	3.27E-02	3.27E-02
8	3.05E-02	3.05E-02	3.11E-02	3.11E-02	3.17E-02	3.17E-02	3.23E-02	3.23E-02
10	3.04E-02	3.05E-02	3.12E-02	3.11E-02	3.19E-02	3.19E-02	3.26E-02	3.26E-02

12	3.07E-02	3.06E-02	3.15E-02	3.15E-02	3.23E-02	3.23E-02	3.32E-02	3.32E-02
15	3.14E-02	3.12E-02	3.23E-02	3.23E-02	3.33E-02	3.31E-02	3.42E-02	3.42E-02
20	3.27E-02	3.24E-02	3.38E-02	3.35E-02	3.49E-02	3.45E-02	3.60E-02	3.57E-02

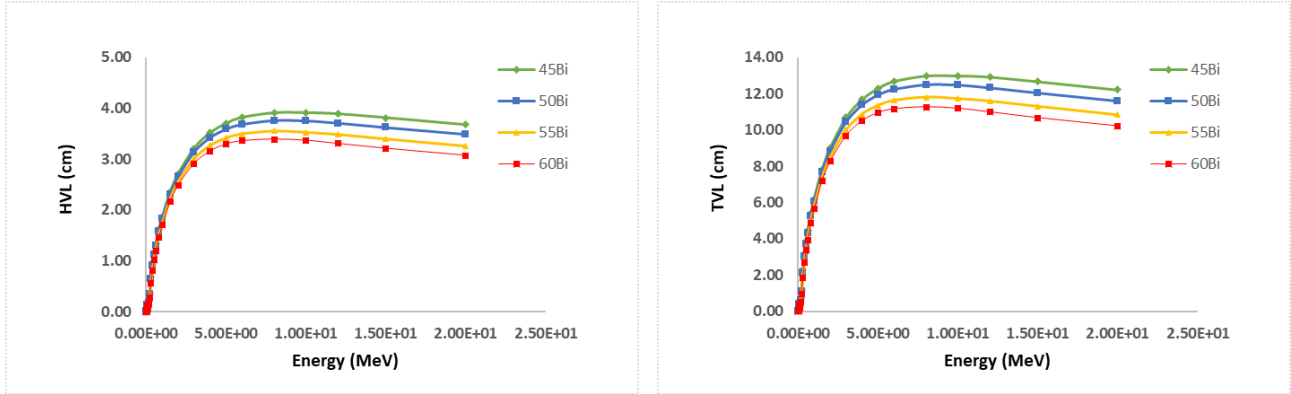


Figure 5. HVL and TVL (cm) in terms of photon energy for glasses.

Figure 6 shows that for the four cases analyzed in this study, the results obtained from GAMOS and XCOM agree with each other by <0.5%.

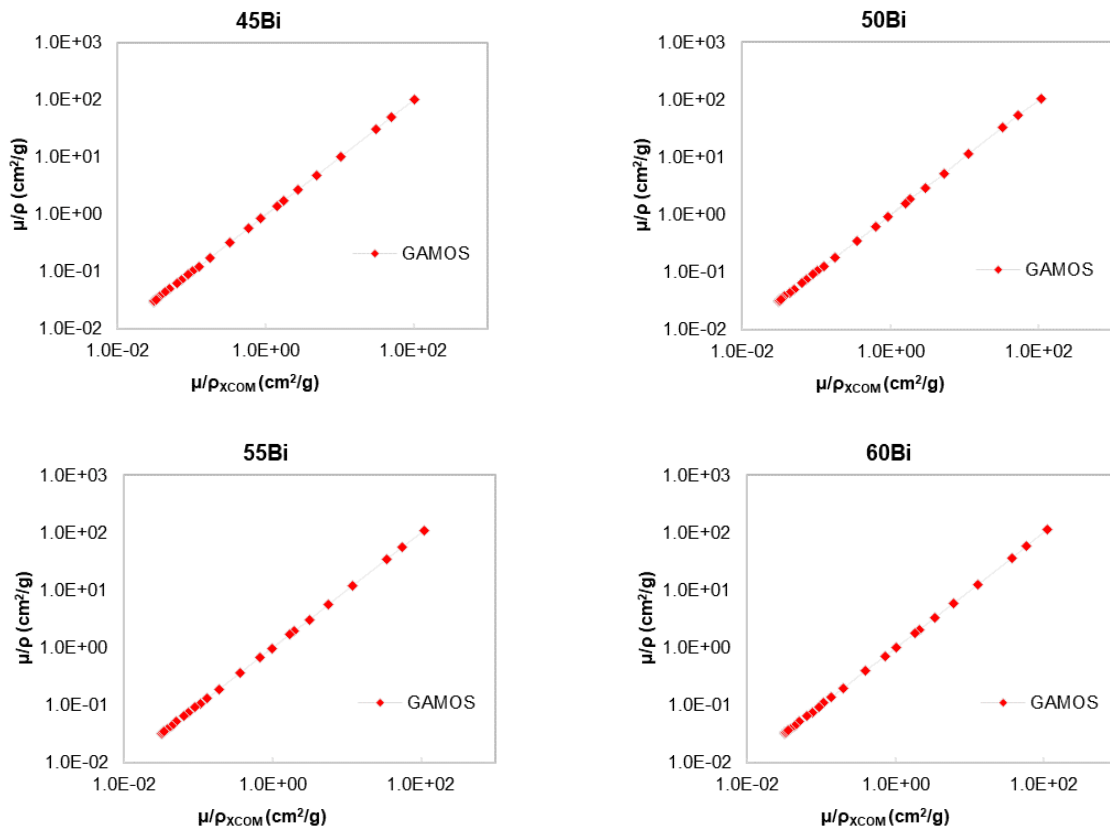


Figure 6. MAC (cm<sup>2</sup>/g) of glasses obtained from Monte Carlo simulations (GAMOS) plotted against data from XCOM database.

#### 4. Conclusion and Suggestions

This study presents a Monte Carlo method to calculate the MAC of  $\text{Bi}_2\text{O}_3\text{-SiO}_2\text{-B}_2\text{O}_3$  glass with varying quantities of  $\text{Bi}_2\text{O}_3$ . The shielding properties of ionizing radiation, such as LAC, MAC, HVL, TVL and MFP, were investigated for glasses in the photon energy range of 0.01-20 MeV. The Monte Carlo simulations yielded results that are in excellent agreement with theoretical data, suggesting that this technique can be used for calculating interaction parameters for materials of interest. Increasing the  $\text{Bi}_2\text{O}_3$ , even in small amounts, had a significant effect on the attenuation of radiation performance. The attenuation coefficients of the selected materials, namely HVL, TVL, and MFP, increase with photon energy. Therefore, these materials are more effective in attenuating low-energy photons.

This approach can serve as an alternative when measuring attenuation coefficients is challenging due to the unavailability of certain gamma energies or difficulties in producing physical

samples. This tool enables the generation of attenuation coefficient data for any given photon energy and material thickness.

#### Contributions of the Authors

The methodology was creating, findings were interpreted, and the article was written by A.S. The idea was developed, the findings were interpreted, and the article was written by İ. A.

#### Conflict of Interest Statement

There is no conflict of interest between the authors.

#### Statement of Research and Publication Ethics

The study is complied with research and publication ethics

#### References

- [1] M. S. Al-Buriahi, H. Arslan, and B. T. Tonguç, "Mass attenuation coefficients, water and tissue equivalence properties of some tissues by Geant4, XCOM and experimental data," *Indian Journal of Pure & Applied Physics (IJPAP)*, vol. 57, no. 6, pp. 433-437, 2019, doi: 10.56042/ijpap.v57i6.22878.
- [2] M. E. Phelps, E. J. Hoffman, and M. M. Ter-Pogossian, "Attenuation coefficients of various body tissues, fluids, and lesions at photon energies of 18 to 136 keV," *Radiology*, vol. 117, no. 3, pp. 573-583, 1975, doi: 10.1148/117.3.573.
- [3] O. Gencel, A. Bozkurt, E. Kam, A. Yaras, E. Erdogmus, and M. Sutcu, "Gamma and neutron attenuation characteristics of bricks containing zinc extraction residue as a novel shielding material," *Progress in Nuclear Energy*, vol. 139, p. 103878, 2021.
- [4] J. H. Hubbell, "Review and history of photon cross section calculations," *Physics in Medicine & Biology*, vol. 51, no. 13, p. R245, 2006.
- [5] A. Sengul *et al.*, "Computation of the impact of NiO on physical and mechanical properties for lithium nickel phosphate glasses," *Journal of Radiation Research and Applied Sciences*, vol. 16, no. 4, p. 100737, 2023/12/01/ 2023, doi:
- [6] N. Karpuz, "Radiation shielding properties of glass composition," *Journal of Radiation Research and Applied Sciences*, vol. 16, no. 4, p. 100689, 2023/12/01/ 2023, doi:
- [7] O. V. Gul, N. Buyukcizmeci, and H. Basaran, "Dosimetric evaluation of three-phase adaptive radiation therapy in head and neck cancer," *Radiation Physics and Chemistry*, vol. 202, p. 110588, 2023.
- [8] O. V. Gul, "Experimental evaluation of out-of-field dose for different high-energy electron beams and applicators used in external beam radiotherapy," *Radiation Physics and Chemistry*, vol. 215, p. 111345, 2024.
- [9] G. Bayrak and H. Müştak, "The Characterization of Welded AA 5005 Alloy with AA 5356 Filler Metals According to Slow Welding Rate Using by MIG Welding Technique," *International Journal of Computational and Experimental Science and Engineering*, vol. 9, no. 4, pp. 346-353, 2023.
- [10] T. Şahmaran and T. Tuğrul, "Investigation of Shielding Parameters of Fast Neutrons for Some Chemotherapy Drugs by Different Calculation Methods," *International Journal of Computational and Experimental Science and Engineering*, vol. 9, no. 4, pp. 388-393, 2023.

- [11] E. Ermis, F. Pilicer, E. Pilicer, and C. Celiktas, "A comprehensive study for mass attenuation coefficients of different parts of the human body through Monte Carlo methods," *Nuclear Science and Techniques*, vol. 27, no. 3, p. 54, 2016, doi: 10.1007/s41365-016-0053-2.
- [12] H. O. Tekin, V. P. Singh, E. E. Altunsoy, T. Manici, and M. I. Sayyed, "Mass attenuation coefficients of human body organs using MCNPX Monte Carlo code," *Iranian Journal of Medical Physics*, vol. 14, no. 4, pp. 229-240, 2017.
- [13] A. Sahin and A. Bozkurt, "Monte Carlo Calculation of Mass Attenuation Coefficients of Some Biological Compounds," *Süleyman Demirel Üniversitesi Fen Edebiyat Fakültesi Fen Dergisi*, vol. 14, no. 2, pp. 408-417.
- [14] A. Bozkurt and A. Sahin "Monte Carlo Approach for Calculation of Mass Energy Absorption Coefficients of Some Amino Acids," *Nuclear Engineering and Technology*, 2021.
- [15] A. Şengül and A. Bozkurt, "Bazı Biyolojik Bileşiklerin Kütleli Enerji Soğurma Katsayılarının Monte Carlo Yöntemiyle Hesaplanması," *Süleyman Demirel Üniversitesi Fen Edebiyat Fakültesi Fen Dergisi*, vol. 16, no. 2, pp. 416-423, 2021.
- [16] I. Akkurt, A. Alomari, M. Y. Imamoglu, and I. Ekmekçi, "Medical radiation shielding in terms of effective atomic numbers and electron densities of some glasses," *Radiation Physics and Chemistry*, vol. 206, p. 110767, 2023.
- [17] R. B. Malidarre, I. Akkurt, O. Kocar, and I. Ekmekci, "Analysis of radiation shielding, physical and optical qualities of various rare earth dopants on barium tellurite glasses: A comparative study," *Radiation Physics and Chemistry*, vol. 207, p. 110823, 2023.
- [18] G. AlMisned, G. Bilal, D. S. Baykal, F. T. Ali, G. Kilic, and H. O. Tekin, "Bismuth (III) oxide and boron (III) oxide substitution in bismuth-boro-zinc glasses: A focusing in nuclear radiation shielding properties," *Optik*, vol. 272, p. 170214, 2023.
- [19] A. Sengul, M. S. Akhtar, I. Akkurt, R. B. Malidarre, Z. Er, and I. Ekmekci, "Gamma-neutron shielding parameters of (S3Sb2) x (S2Ge) 100– x chalcogenide glasses nanocomposite," *Radiation Physics and Chemistry*, vol. 204, p. 110675, 2023.
- [20] A. Şengül, "Gamma-ray attenuation properties of polymer biomaterials: Experiment, XCOM and GAMOS results," *Journal of Radiation Research and Applied Sciences*, vol. 16, no. 4, p. 100702, 2023.
- [21] A. Şengül, "ZnO Katkılı Bazı Cam Örneklerinin Kütle Zayıflama Katsayılarının Monte Carlo ile Hesaplanması," *Dokuz Eylül Üniversitesi Mühendislik Fakültesi Fen ve Mühendislik Dergisi*, vol. 25, no. 75, pp. 751-759.
- [22] O. V. Gul and M. Duzova, "Effect of different CTV shrinkage and skin flash margins on skin dose for left chest wall IMRT: A dosimetric study," *Radiation Physics and Chemistry*, vol. 216, p. 111445, 2024.
- [23] A. Coşkun, B. Çetin, İ. Yiğitoğlu, and B. Canimkurbey, "Theoretical and Experimental Investigation of Gamma Shielding Properties of TiO<sub>2</sub> and PbO Coated Glasses," *International Journal of Computational and Experimental Science and Engineering*, vol. 9, no. 4, pp. 398-401, 2023.
- [24] M. Berger *et al.*, "XCOM: Photon Cross Sections Database. NIST, PML, Radiation Physics Division," ed, 2019.
- [25] J. K. Shultis and R. E. Faw, *Fundamentals of Nuclear Science and Engineering*. CRC Press, 2016.
- [26] H. O. Tekin, V. P. Singh, and T. Manici, "Effects of micro-sized and nano-sized WO<sub>3</sub> on mass attenuation coefficients of concrete by using MCNPX code," *Applied Radiation and Isotopes*, vol. 121, pp. 122-125, 2017.
- [27] G. Hongwei *et al.*, "Microstructures and properties of (65-x) SiO<sub>2</sub>-xBi<sub>2</sub>O<sub>3</sub>-10B<sub>2</sub>O<sub>3</sub>-25CuO glasses," *Journal of Non-Crystalline Solids*, vol. 569, p. 120972, 2021.
- [28] H. Masai, M. Takahashi, Y. Tokuda, and T. Yoko, "Gel-melting method for preparation of organically modified siloxane low-melting glasses," *Journal of materials research*, vol. 20, pp. 1234-1241, 2005.
- [29] S. K. Hong, H. Y. Koo, Y. N. Ko, J. H. Kim, J. H. Yi, and Y. C. Kang, "Eu-doped B<sub>2</sub>O<sub>3</sub>-ZnO-PbO glass phosphor powders with spherical shape and fine size prepared by spray pyrolysis," *Applied Physics A*, vol. 98, pp. 671-677, 2010.
- [30] I. Dyamant, D. Itzhak, and J. Hormadaly, "Thermal properties and glass formation in the SiO<sub>2</sub>-B<sub>2</sub>O<sub>3</sub>-Bi<sub>2</sub>O<sub>3</sub>-ZnO quaternary system," *Journal of non-crystalline solids*, vol. 351, no. 43-45, pp. 3503-3507, 2005.

- [31] V. Golubkov, P. Onushchenko, and V. Stolyarova, "Studies of glass structure in the system Bi<sub>2</sub>O<sub>3</sub>-B<sub>2</sub>O<sub>3</sub>-SiO<sub>2</sub>," *Glass Physics and Chemistry*, vol. 41, pp. 247-253, 2015.
- [32] Y. Gao, J.-J. Ma, Y. Chen, and M.-H. Wang, "Effect of Bi<sub>2</sub>O<sub>3</sub> on the structure and thermal properties of Bi<sub>2</sub>O<sub>3</sub>-SiO<sub>2</sub>-B<sub>2</sub>O<sub>3</sub> glasses prepared by sol-gel method," *Journal of Sol-Gel Science and Technology*, vol. 103, no. 3, pp. 713-721, 2022.
- [33] B. Oruncak, "Computation of Neutron Coefficients for B<sub>2</sub>O<sub>3</sub> reinforced Composite," *International Journal of Computational and Experimental Science and Engineering*, vol. 9, no. 2, pp. 50-53.
- [34] P. Arce, P. Rato, M. Canadas, and J. I. Lagares, "GAMOS: A Geant4-based easy and flexible framework for nuclear medicine applications," in *2008 IEEE Nuclear Science Symposium Conference Record*, 2008: IEEE, pp. 3162-3168.
- [35] P. Andreo, "Monte Carlo techniques in medical radiation physics," *Physics in Medicine & Biology*, vol. 36, no. 7, p. 861, 1991.
- [36] S. Agostinelli *et al.*, "GEANT4—a simulation toolkit," *Nuclear instruments and methods in physics research section A: Accelerators, Spectrometers, Detectors and Associated Equipment*, vol. 506, no. 3, pp. 250-303, 2003.